Development of constriction resistance model for dropwise condensation using drop-size distribution characteristics

Jae Young Choi [a], Yong Hoon Jeong [a*]
a: Department of Nuclear & Quantum Engineering, Korea Advanced Institute of Science and Technology (KAIST)
291 Daehak-ro, Yuseong-gu, Daejeon, 34141, Korea
*: Corresponding author: jeongyh@kaist.ac.kr

1. Introduction

Dropwise condensation (DWC) were first recognized by Schmidt et al. Typically, DWC was known as high heat transfer coefficient which has 5~7 times higher that of filmwise condensation (FWC). Several papers reported that DWC phenomena can be observed on stainless steel or coated substrate by hydrophobic material, and utilization of dropwise condensation has an opportunity to reduce the heat exchanger size when we design safety system for PCCS.

In the presence of droplet on the vertical cooling surface, the thermal resistance model for DWC is different from that of FWC. Overall resistance for DWC is consists of interfacial resistance, capillary depression resistance, droplet conduction resistance and constriction resistance. Table I shows the previous study on thermal resistance models for DWC [1–6]. The notaion of parameters, Ri, Rcap, Rdrop, Rs, and θ are interfacial resistance, capillary depression resistance, drop conduction resistance, constriction resistance and surface inclination, respectively. There was a controversy on the constriction resistance model[7]. However, the studies from Mikic[2] and Tsuruta & Tanaka[4,5] found out that there is significant decrease of DWC heat transfer coefficient induced by constriction resistance. Their constriction resistance model assumed that 1) heat transfer through inactive droplet is negligible and 2) there is no discontinuity if droplet number density correlation[1,8] at a droplet radius larger than 0.2 times of its departure radius[9]. Therefore, the objective of this paper is to develop DWC with the consideration of constriction resistance model and to reflect the effect of using realistic drop-size distribution.

Table I: Summary of existing DWC models

Models	Ri	Rcap	Rdrop	Rs	θ
Le Fevre & Rose (1966)	O	O	O	X	90o
Mikic (1969)	O	X	O	O	90o
Tanaka (1975)	O	X	O	X	90o
Tsuruta & Tanaka (1990)	O	X	O	O	90o
Abu-Orabi (1998)	O	O	O	X	90o
Bonner III (2013)	O	O	O	X	0~90o

2. Methods

2.1 Experimental Method

A schematic diagram of the experimental loop and test section are shown in Fig. 1. Four K-type sheathed thermocouples(accuracy: ±0.1 K, and response time: less than 4 ms) were mounted in the SUS316 cooling surface with different depth from the outer surface (1, 2, 3, and 4 ± 0.005 mm). In addition, the cooling surface was observed by a high-speed camera at a right angle to quantify the drop-size distribution parameters. All experiments were conducted in atmospheric pressure. The experimental results for subcooled temperature (1~30K) and non-condensable gas concentration (0~40%) were observed.

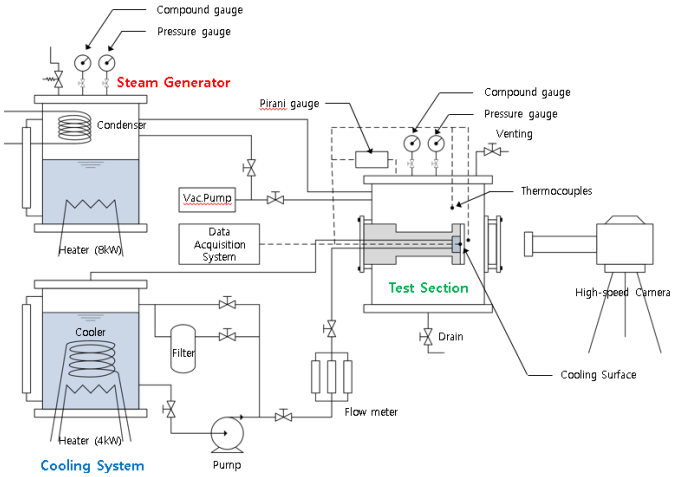

Fig.1. Schematic of the experimental apparatus

2.2 Droplet Visualization

The original images (1024 x 1024 pixels, 8-bit gray-scale images, bitmap file) have been obtained at each experimental conditions. The images were recorded with three different magnifications: x 2.28, x16.0, and 36.8. Each magnification can measure the droplets with the radius range of over 100 microns, 40 ~ 1000 microns, and 10 ~ 500 microns, respectively. To quantify the drop-size distribution, contrast, sharpening, binarization, filtering and drop size correction were processed in order as shown in Fig.2. At last, 512 x 512 pixels in the center of processed images were inspected for accurate measuring regardless of observed droplet size.

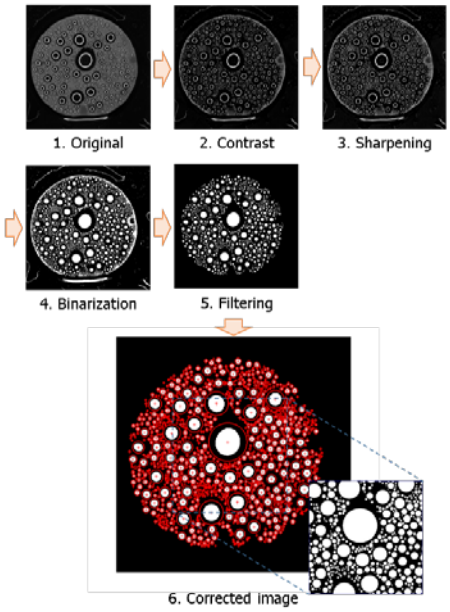

Fig. 2. Procedures of image processing

3. Results and Discussions

3.1 Drop-size distribution

Maximum droplet departure radius was obtained from all experimental condition as shown in Fig. 3.

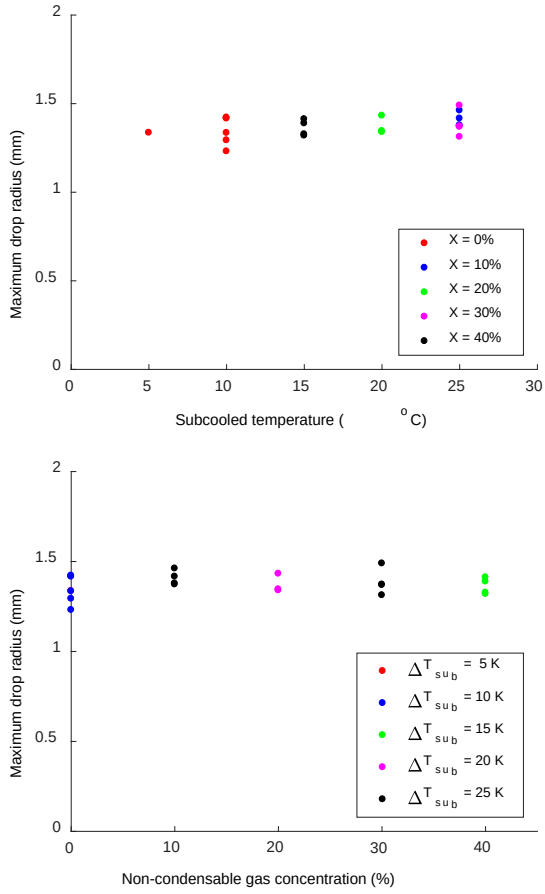

Fig. 3. Maximum droplet departure radius

Upper and lower figure show the effect of subcooled temperature and non-condensable gas, respectively. As we can notice from the results, the maximum drop departure radius was measured to be 1.37mm for SUS316 surface regardless of experimental conditions.

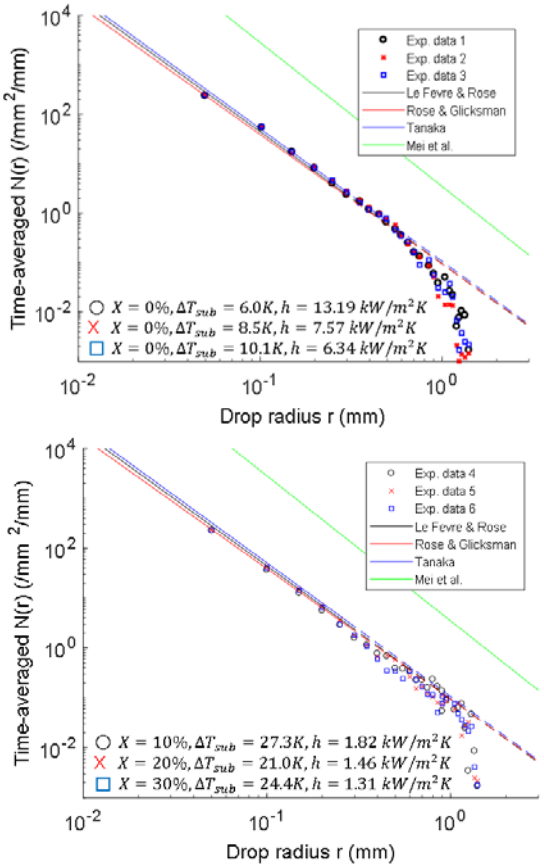

Fig. 4. Drop-size distribution density (time-averaged)

Various drop-size distribution functions versus drop radius were observed. The basic parameter to express the state of droplet distribution is drop-size distribution density $\bar{N}(r)$. In Fig. 4. The correlation derived by other researchers are fitted in the graph. Those correlations were well-fitted to the experimental data at small drop radius region. However, breakaway from the correlation was observed for droplet radius larger than 0.2 times of its maximum departure radius. Therefore, current drop-size distribution study over-estimated the number of large droplets, which lead to high constriction resistance.

As like as the measurement of maximum departure radius in Fig. 3., the drop-size distribution density $\bar{N}(r)$ is independent to the experimental condition.

The time-averaged fraction of the area covered by drops with larger than r $\bar{f}(r)$ is shown in Fig. 5. By the definition of $\bar{f}(r)$, the function can be expressed as:

$$f(r) = \int_r^{r_{max}} \pi r^2 N(r) dr \qquad (1)$$

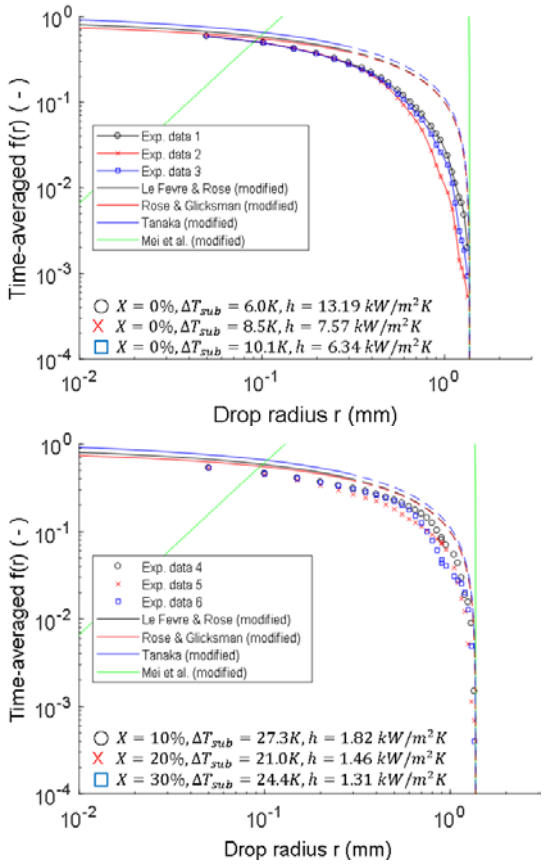

Fig. 5. Fraction of the area covered by drops with larger than r (time-averaged)

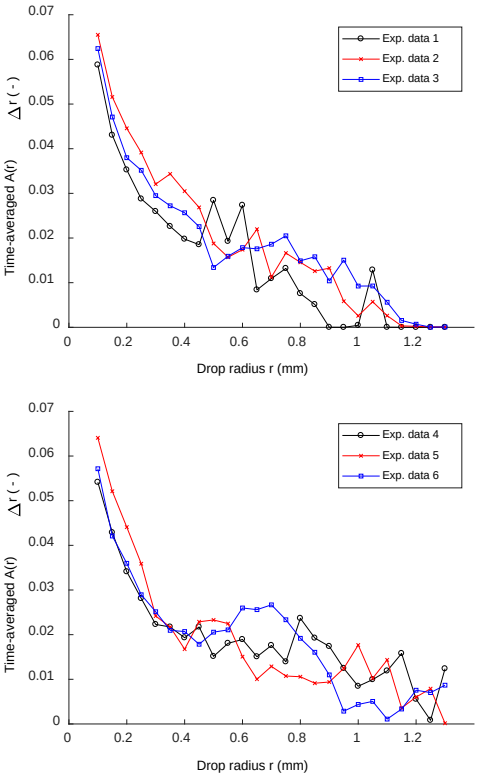

Fig. 6. Area coverage fraction from r to r+Δr (time-averaged)

By Rose & Glicksman's model, $\bar{f}(r_{min})$ reaches to 0.78. Similar to $\bar{N}(r)$, existing $\bar{f}(r)$ correlations show also bad estimation for large droplet larger than 0.2 times of its maximum departure radius. Moreover, the time-averaged area coverage fraction within $[\,r\ r+\Delta r\,]$, $\bar{A}(r)\Delta r$, is presented in Fig.6. (Δr = 0.05 mm)

3.2 Model Development

The model for the single elemental channel, described in Fig. 7., was derived. The heat conduction equation and corresponding boundary conditions were described as:

$$\nabla^2 T = \frac{\partial^2 T}{\partial r^2} + \frac{1}{r}\frac{\partial T}{\partial r} + \frac{\partial^2 T}{\partial z^2} = 0 \tag{2}$$

$$-k_s\left(\frac{\partial T}{\partial z}\right) = \frac{Q_d}{\pi r_d^2} \quad \text{at } z = 0 \text{ and } 0 < r < r_d \tag{3}$$

$$-k_s\left(\frac{\partial T}{\partial z}\right) = \frac{Q_a}{\pi(r_a^2 - r_d^2)} \quad \text{at } z = 0 \text{ and } r_d \le r < r_a \tag{4}$$

$$-k_s\left(\frac{\partial T}{\partial z}\right) = \frac{Q_a + Q_d}{\pi r_a^2} \quad \text{at } z \to \infty \tag{5}$$

$$-k_s\left(\frac{\partial T}{\partial r}\right) = 0 \quad \text{at } r = 0 \text{ and } r_a \tag{6}$$

By solving equation (2)~(6), the analytic solution for local surface temperature $T_c(r)$, and weighted mean surface temperature T_{cm} is:

$$T_c = \overline{T}_s + \frac{2r_d}{k_s}\left(\frac{Q_d}{A_d} - \frac{Q_a}{A_a}\right)\sum_{n=1}^{\infty}\frac{J_1(\alpha_n r_d)J_0(\alpha_n r)}{(\alpha_n r_a)^2 J_0^2(\alpha_n r_a)} \tag{7}$$

$$T_{cm} = \overline{T}_s + \frac{4\pi}{k_s}\left(\frac{Q_a}{A_a} - \frac{Q_d}{A_d}\right)\frac{r_a r_d^2}{A_a}\sum_{n=1}^{\infty}\frac{J_1^2(\alpha_n r_d)}{(\alpha_n r_a)^3 J_0^2(\alpha_n r_a)} \tag{8}$$

Then, by the definition of constriction resistance,

$$R_s = \frac{4\pi}{k_s}\left(\frac{X_{Q,a}}{A_a} - \frac{X_{Q,d}}{A_d}\right)\frac{r_d^3}{A_a}\psi = \frac{4}{k_s}\left(\frac{X_{Q,a}}{A_a} - \frac{X_{Q,d}}{A_d}\right)\frac{A_d}{A_a}\psi r_d \tag{9}$$

Where,

$$\psi = \frac{r_a}{r_d}\sum_{n=1}^{\infty}\frac{J_1^2(\alpha_n r_d)}{(\alpha_n r_a)^3 J_0^2(\alpha_n r_a)} \cong \frac{2}{3\pi}\left(1 - \frac{r_d}{r_a}\right)^{1.5} \tag{10}$$

$$X_{Q,a} \equiv \frac{Q_a}{Q_a + Q_d}, X_{Q,d} \equiv \frac{Q_d}{Q_a + Q_d} \tag{11}$$

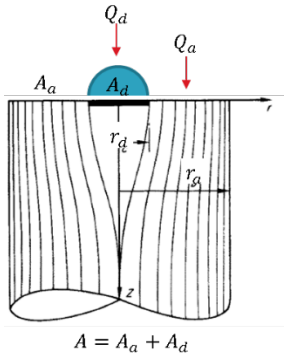

Fig. 7. A schematic of the elemental heat channel

Derived constriction resistance model can be expanded to multiple droplet surface. By the proper approximation, ($r_d \to r$, $R_s = R_s' dr$, $\frac{A_d}{A_a^2} \cong \frac{A(r)dr}{(1-f(r))^2}$)

$$R_s = \int R_s'(r)dr = \int_{r_{min}}^{r_{max}} \frac{4}{k_s} \Delta X_Q \psi \frac{A(r)}{\left(1-f(r)\right)^2} r dr \quad (12)$$

And overall heat transfer coefficient considering four thermal resistances can be expressed as:

$$h^{-1} = \frac{A_{total}}{4\pi k_l} \frac{1}{\sum_i \frac{4\pi k_l r}{1+\frac{2k_l}{h_i r}}\left(1-\frac{r_{cri}}{r}\right)} + \frac{1.188}{k_s} \int_{r_{min}}^{r_{max}} \frac{A(r)}{\left(1-f(r)\right)^2} r dr \quad (13)$$

4. Conclusions

In this study, drop-size distribution parameters were quantified and new constriction resistance model was developed. All drop-size distribution, including droplet number density, fraction of the area covered by drops with larger than r, and Area coverage fraction from r to r+Δr, are independent to the experimental condition such as subcooled temperature and non-condensable gas concentration. The drop-size distribution parameters are the function of r and r_{max}. The equation for constriction resistance were derived and it considered the heat transfer through inactive droplet and the distribution of large droplets.

REFERENCES

[1] Le Fevre EJ, Rose JW. A theory of heat transfer by dropwise condensation. Chem Eng Prog 1966;62:86.

[2] Mikic BB. On Mechanism of Dropwise Condensation. Int J Heat Mass Transf 1969;12:1311–23.

[3] Tanaka H. A Theoretical Study of Dropwise Condensation. J Heat Transfer 1975;97:72–8.

[4] Tsuruta T, Tanaka H. A theoretical study on the constriction resistance in dropwise condensation. Int J Heat Mass Transf 1991;34:2779–86. doi:10.1016/0017-9310(91)90237-9.

[5] Takaharu T, Hiroaki T, Shigenori T. Experimental verification of constriction resistance theory in dropwise condensation heat transfer. Int J Heat Mass Transf 1991;34:2787–96. doi:10.1016/0017-9310(91)90238-A.

[6] Bonner RW. Correlation for dropwise condensation heat transfer: Water, organic fluids, and inclination. Int J Heat Mass Transf 2013;61:245–53. doi:10.1016/j.ijheatmasstransfer.2012.12.045.

[7] Rose JW. Dropwise condensation theory and experiment: a review. Proc Inst Mech Eng Part A J Power Energy 2002;216:115–28. doi:10.1243/09576500260049034.

[8] Rose JW, Glicksman LR. Dropwise condensation-The distribution of drop sizes. Int J Heat Mass Transf 1973;16:411–25. doi:10.1016/0017-9310(73)90068-9.

[9] Graham C. The limiting heat transfer mechanisms of dropwise condensation. Massachusetts Institute of Technology, 1969.